ELSEVIER

Catalysis Today 73 (2002) 263–270

CATALYSIS TODAY

www.elsevier.com/locate/cattod

Mean field modelling of NO_x storage on $Pt/BaO/Al_2O_3$

Louise Olsson [a,b,c,*], Erik Fridell [a,c], Magnus Skoglundh [a,d], Bengt Andersson [a,b]

[a] Competence Centre for Catalysis, Chalmers University of Technology, SE-412 96 Göteborg, Sweden
[b] Department of Chemical Reaction Engineering, Chalmers University of Technology, SE-412 96 Göteborg, Sweden
[c] Department of Applied Physics, Chalmers University of Technology, SE-412 96 Göteborg, Sweden
[d] Department of Applied Surface Chemistry, Chalmers University of Technology, SE-412 96 Göteborg, Sweden

Abstract

A mean field model, for storage and desorption of NO_x in a $Pt/BaO/Al_2O_3$ catalyst is developed using data from flow reactor experiments. This relatively complex system is divided into five smaller sub-systems and the model is divided into the following steps: (i) NO oxidation on Pt/Al_2O_3; (ii) NO oxidation on $Pt/BaO/Al_2O_3$; (iii) NO_x storage on BaO/Al_2O_3; (iv) NO_x storage on $Pt/BaO/Al_2O_3$ with thermal regeneration and (v) NO_x storage on $Pt/BaO/Al_2O_3$ with regeneration using C_3H_6. In this paper, we focus on the last sub-system. The kinetic model for NO_x storage on $Pt/BaO/Al_2O_3$ was constructed with kinetic parameters obtained from the NO oxidation model together with a NO_x storage model on BaO/Al_2O_3. This model was not sufficient to describe the NO_x storage experiments for the $Pt/BaO/Al_2O_3$, because the NO_x desorption in TPD experiments was larger for $Pt/BaO/Al_2O_3$, compared to BaO/Al_2O_3. The model was therefore modified by adding a reversible spill-over step. Further, the model was validated with additional experiments, which showed that NO significantly promoted desorption of NO_x from $Pt/BaO/Al_2O_3$. To this NO_x storage model, additional steps were added to describe the reduction by hydrocarbon in experiments with NO_2 and C_3H_6. The main reactions for continuous reduction of NO_x occurs on Pt by reactions between hydrocarbon species and NO in the model. The model is also able to describe the reduction phase, the storage and NO breakthrough peaks, observed in experiments. © 2002 Elsevier Science B.V. All rights reserved.

Keywords: NO_x reduction; NO_x storage; $Pt/BaO/Al_2O_3$; Kinetic modelling

1. Introduction

It is important to reduce the emissions of the greenhouse gas CO_2 by lowering the fuel consumption for gasoline engines. One way to obtain this is to use engines operating with oxygen excess, so-called lean operation. However, a major problem with lean operation is that conventional three way catalysts are not able to reduce the NO_x. One possible solution to this problem is the so-called NO_x storage concept [1–7], where the air–fuel ratio is altered between lean (oxygen excess) and rich (fuel excess) mixtures. During the lean periods, the NO_x is trapped in a specific storage component in the catalyst. During short rich periods the storage material is regenerated and the desorbed NO_x reacts with hydrocarbons and CO to produce CO_2, H_2O and N_2. However, there are also problems with this technique. The major one being sulphur poisoning of the storage component by the formation of sulphates [6]. For improving the sulphur resistance and for optimising the temperature stability, NO_x storage ability, and regeneration times, detailed knowledge about the NO_x storage and regeneration mechanisms is crucial. The NO_x storage concept consists of several different steps: NO oxidation, NO_x storage, regeneration and

---

[*] Corresponding author. Present address: Department of Chemical Reaction Engineering, Chalmers University of Technology, SE-412 96 Göteborg, Sweden. Fax: +46-031-772-3035.
E-mail address: louise@cre.chalmers.se (L. Olsson).

0920-5861/02/$ – see front matter © 2002 Elsevier Science B.V. All rights reserved.
PII: S0920-5861(02)00009-3

formation of carbonates. We have previously investigated NO oxidation on $Pt/BaO/Al_2O_3$ and NO_x storage with thermal regeneration [7]. Burch et al. [8–10] have investigated the kinetics for the reaction between C_3H_6 and NO in oxygen excess, which also are steps that are important in the NO_x storage concept. Further, experimental studies of the importance of carbonate formation can be found in literature [11,12].

The objective of this work is to increase the understanding of the mechanism for NO_x storage on $Pt/BaO/Al_2O_3$ with regeneration by hydrocarbons. Both experimental methods and kinetic modelling are used.

2. Experimental

A $Pt/BaO/Al_2O_3$ monolith catalyst containing 2.0 wt.% Pt and 20 wt.% BaO with a washcoat weight of 204 mg was used. The preparation procedure of the catalyst is described in [4,13,14].

The continuous flow reactor system used is described in detail elsewhere [13,14]. Briefly, it consists of a gas mixing part with several mass flow controllers, a quartz reactor and finally a gas analysing system, where NO and NO_2 are analysed with a chemiluminescence detector (Tecan CLD 700 EL ht), N_2O with an IR-instrument (Maihak, UNOR 610) and CO_2 with an UNOR 6N IR detector. The catalyst was placed in the quartz tube with one thermocouple placed inside the catalyst and another one about 10 mm in front of the catalyst.

NO_x storage with NO, NO_2 and O_2. Several types of experiments were performed. In the first type, the catalyst was exposed to 680 ppm NO_2 at different temperatures for 10 min. The catalyst was then flushed with inert gas for 5 min, followed by a temperature ramp (20 °C/min). This experiment was repeated, but after the NO_2 adsorption, there was only 1 min with inert gas in the flow, followed by 4 min with 600 ppm NO/N_2. The temperature ramp was also conducted with 600 ppm NO in the flow. These two types of experiments were conducted at 300 and 350 °C. The third type of experiment comprised oxygen transients. At 350 and 400 °C the catalyst was exposed to 600 ppm NO and 5 min intervals of oxygen at different concentrations (8, 0, 4, 0, 1, 0% O_2). The flow rate was 2600 ml/min.

NO_x storage with NO_2 and C_3H_6. In these experiments the concentration of NO_2 was 500 ppm, and the C_3H_6 concentration was altered between 0 and 1000 ppm in 5 min intervals. This experiment was performed for three temperatures: 300, 400 and 500 °C, respectively. The flow rate was 3000 ml/min.

3. Theory

The kinetic model is a mean field model. The monolith is described by a series of continuous stirred tanks. Many of the parameters in the model were kept fixed to literature values [7], while others were fitted with the least-squares method. For the NO_x storage experiments with NO_2 only, and for the NO oxidation model, 15 tanks were used. For the model including hydrocarbons, 10 tanks were used due to time limitations. In these experiments about 13 500 data points were used and the total model is large. However, there was only a small difference in the regression sum of squares between using 10 or 15 tanks. According to transition state theory [15], the maximum value for pre-exponential factors for Langmuir–Hinshelwood reactions is $10^{19}\ s^{-1}$, and therefore this limit was used in the fitting procedure.

The main idea in building this model is to make experiments on a smaller system first to obtain values for some parameters, which then are kept fixed through the rest of the modelling. Accordingly, a model for oxygen adsorption/desorption on Pt/Al_2O_3 was initially constructed. With the use of the parameters obtained from this model a NO oxidation model for Pt/Al_2O_3 and $Pt/BaO/Al_2O_3$ was then constructed [7]. The NO_x storage model for BaO/Al_2O_3 was then made, which in turn was used together with the NO oxidation model to create a NO_x storage model for $Pt/BaO/Al_2O_3$ [7], which is summarised below. Finally, we have used this model, with all parameters kept fixed, to build the NO_x storage model including regeneration with propene. Most of the reaction steps used for regeneration with propene are summation reactions, which may include several surface species. The reason for this is that to use only elementary steps would give an enormous amount of steps and unknown kinetic parameters. The objective with this part of the model was to make the model as simple as possible and therefore physical interpretations of the kinetic parameters for the propene regeneration should not be made.

4. Results and discussion

4.1. NO_x storage on $Pt/BaO/Al_2O_3$—without reducing agent

A kinetic model for NO_x storage on BaO was constructed by using five reversible reactions. Details regarding this model can be found in [7]. In the model NO_2 is first adsorbed on a BaO site, which is denoted S_1. In experiments where a BaO/Al_2O_3 catalyst is exposed to NO_2, an initial formation of NO is seen [5]. The reason for this may be that the surface or species on the surface are oxidised by NO_2, resulting in NO formation. In the model, we have therefore added a step where the adsorbed NO_2 dissociates to $NO_{(g)}$ and leaves an oxygen atom on the surface:

$$NO_{2(g)} + S_1 \underset{r_2}{\overset{r_1}{\rightleftarrows}} S_1\text{–}NO_2 \tag{1}$$

$$S_1\text{–}NO_2 \underset{r_4}{\overset{r_3}{\rightleftarrows}} S_1\text{–}O + NO_{(g)} \tag{2}$$

On this oxide (i.e. oxidised or oxygen covered site), we allow NO_2 to adsorb and form a nitrate. From experiments with NO_2 exposure on BaO/Al_2O_3 at 500 °C, it was seen that NO_2 continuously dissociated to NO, and thus also O_2 had to be formed. It was therefore necessary to include a step where $O_{2(g)}$ was formed. These two reaction steps are shown below

$$NO_{2(g)} + S_1\text{–}O \underset{r_6}{\overset{r_5}{\rightleftarrows}} S_1\text{–}NO_3 \tag{3}$$

$$2S_1\text{–}O \underset{r_8}{\overset{r_7}{\rightleftarrows}} 2S_1 + O_{2(g)} \tag{4}$$

From the previously mentioned experiment with NO_2 exposure on the BaO/Al_2O_3 catalyst, it was seen that the amount of reacted NO_2 was three times as large as the formation of NO. This is in agreement with another study performed by Cant and Patterson [16]. The stoichiometry in our model was $3NO_2$ reacted for each NO formed and we therefore assumed that NO_2 can adsorb both on the barium and the oxygen part of BaO and added the following step:

$$NO_{2(g)} + S_1\text{–}NO_3 \underset{r_{10}}{\overset{r_9}{\rightleftarrows}} Ba(NO_3)_2 \tag{5}$$

This model was able to describe the experiments well and the results can be found in [7].

The NO_x storage model was used together with a NO oxidation model [7,13] and tested with experiments using a $Pt/BaO/Al_2O_3$ catalyst and with all parameters kept fixed. The experimental sequence used when testing the model was an exposure of the catalyst to 680 ppm NO_2 at 300 or 350 °C, followed by 5 min of inert gas and finally a temperature ramp in inert gas. The model could not sufficiently describe the experiments, since NO_2 was found to desorb at lower temperatures in experiments with platinum present. Therefore, we tried to describe this behaviour with a spill-over mechanism of NO_2 from platinum- to barium-sites and reverse. A spill-over mechanism has previously been used by Burch and Watling [8] to describe the reactions between propane and NO_x on Pt/Al_2O_3. In that case NO_2 spills over to the support, where it reacts with adsorbed hydrocarbon species. Only one spill-over step was necessary to describe our experiments, which was added to the model

$$Pt\text{–}NO_2 + S_1\text{–}NO_3 \underset{r_{12}}{\overset{r_{11}}{\rightleftarrows}} Ba(NO_3)_2 + Pt \tag{6}$$

Four transient experiments were used to determine the kinetic parameters and the values can be found in [7].

The model was validated with separate experiments not included in the fitting procedure. The experimental sequence in these experiments was: NO_2 adsorption (at 300 or 350 °C) followed by 1 min with N_2 and 4 min with NO/N_2 and finally a temperature ramp. In Fig. 1, the NO_x concentrations from both the 350 °C experiment used in the fitting and the validation experiment (with NO at 350 °C) are given. The solid lines are the experimental concentrations and the dotted lines the calculated. There was a rapid desorption of NO_x when NO was switched on. This rapid desorption is in the model explained by that $NO_{(g)}$ adsorbs on platinum and reacts with oxygen on the Pt surface forming NO_2, which desorbs. The coverage of oxygen on the Pt surface decreases, due to the reaction with NO on platinum, which results in an increased spill-over of NO_x from the barium- to the platinum-sites.

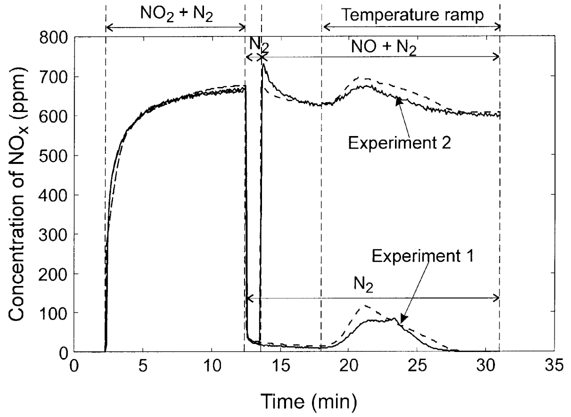

Fig. 1. The outlet concentration of NO_x from two experiments at 350 °C. The experiments are represented with solid lines and the simulations with dotted lines. Experiment 1 (used in fitting): 10 min of 680 ppm NO_2 in N_2, 5 min N_2, temperature ramp in N_2. Experiment 2 (validation experiment): 10 min of 680 ppm NO_2 in N_2, 1 min N_2, 4 min in 600 ppm NO/N_2, temperature ramp in NO/N_2.

4.2. NO_x storage on $Pt/BaO/Al_2O_3$—with propene as reducing agent

Transient experiments with alternating 5 min of NO_2 and 5 min of $NO_2 + C_3H_6$ at two temperatures, 300 and 400 °C, were used to construct a kinetic model for the reduction of NO_x in the NO_x storage process. The upper panels of Figs. 2 and 3 show the experimental concentrations of NO, NO_2, NO_x and CO_2. From the experiments, it can be observed that during the reducing period ($NO_2 + C_3H_6$) the conversion of NO_x to N_2 is complete at 400 °C, but not at 300 °C. Further, when the lean mixture (NO_2) is switched on a storage of NO_x is seen and the concentration of NO_x slowly increases. Finally, when the gas mixture is changed to rich a NO breakthrough peak is observed in the experiment [4,5], where the NO concentration for a short time exceeds the inlet concentration of NO_x. Also shown in Figs. 2 and 3 are the results from the modelling, which will be discussed below. All parameters from the NO_x storage model described above, including NO oxidation, number of sites, etc. were kept fixed and only parameters for steps involving hydrocarbons were fitted.

It can be found in the literature that the main reaction pathway for NO_x reduction on Pt/Al_2O_3 depends on the type of reducing agent used [8,18]. For propene, the reaction occurs mainly on active platinum-sites and involves reduction of NO, and the formation of NO_2 does not seem to be crucial. However, if propane

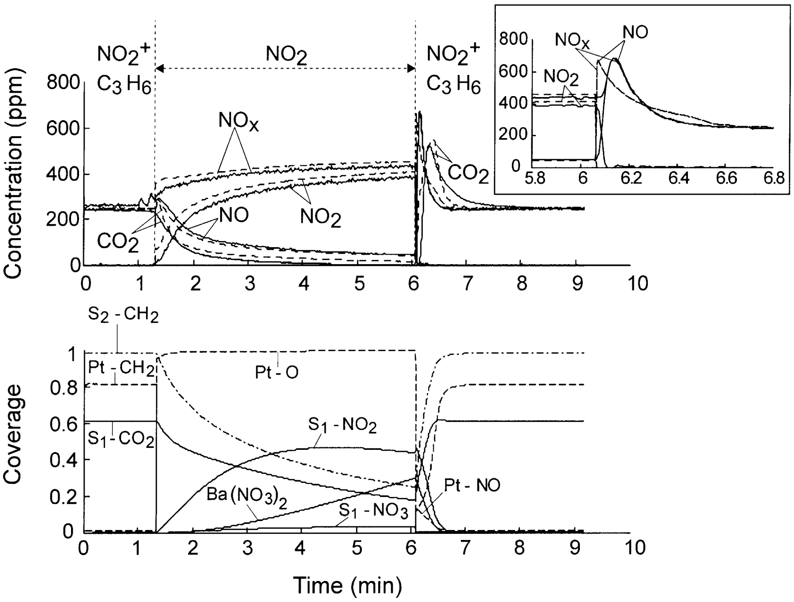

Fig. 2. Upper panel: the outlet concentrations of NO, NO_2, NO_x and CO_2 according to the experiment (solid line) and the kinetic model (dotted line). The $Pt/BaO/Al_2O_3$ catalyst was exposed to 500 ppm NO_2 and alternating C_3H_6 concentrations (1000, 0, 1000 ppm) at 300 °C. A magnification of the breakthrough peak in NO is also shown. Lower panel: the calculated coverages on the surface.

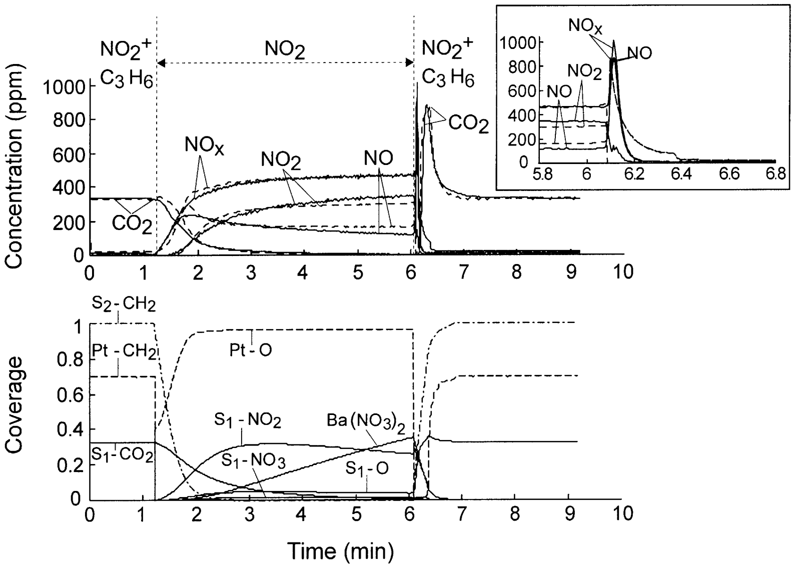

Fig. 3. Upper panel: the outlet concentrations of NO, NO_2, NO_x and CO_2 according to the experiment (solid line) and the kinetic model (dotted line). The $Pt/BaO/Al_2O_3$ catalyst was exposed to 500 ppm NO_2 and alternating C_3H_6 concentrations (1000, 0, 1000 ppm) at 400 °C. A magnification of the breakthrough peak in NO is also shown. Lower panel: the calculated coverages on the surface.

is used the mechanism is reported to be different. The most important role of platinum in this case seems to be to oxidise NO to NO_2, which, after spill-over to the support, reacts with adsorbed hydrocarbon species [8]. Since only propene was used in the present experiments a reaction involving hydrocarbons and NO on platinum was used as the base for our mechanism. In the first step C_3H_6 is adsorbed on platinum. It is likely that propene dissociates on this surface to various types of hydrocarbon species [8]. To describe all details of the hydrocarbon chemistry would be very complex. To simplify the model, we have used $–CH_2$ as the hydrocarbon species formed from propene decomposition over platinum. The reason for choosing $–CH_2$ was that from C_3H_6 there would be three identical CH_2 species and if, e.g. CH or CH_3 had been chosen it would in the model been necessary to use several CH_x species on the surface, which would have given a very complex model. Further, spectroscopic evidence for $–CH_2$ adsorbed on Pt(1 1 1) is reported [17]. The following two reactions describes this HC formation:

$$C_3H_{6(g)} + Pt \underset{r_{14}}{\overset{r_{13}}{\rightleftarrows}} Pt–C_3H_6 \tag{7}$$

$$Pt–C_3H_6 + 2Pt \xrightarrow{r_{15}} 3Pt–CH_2 \tag{8}$$

In the model, summary reactions are used both for the oxidation of CH_2 and for the reduction of NO by CH_2 over platinum. The reason for using these summary reactions, is to decrease the number of reactions and thereby the number of free parameters needed to be fitted. The following two reactions were used:

$$Pt–CH_2 + 3Pt–O \xrightarrow{r_{16}} 4Pt + CO_{2(g)} + H_2O_{(g)} \tag{9}$$

$$Pt–CH_2 + 3Pt–NO \xrightarrow{r_{17}} 4Pt + CO_{2(g)} + H_2O_{(g)} + 1.5N_{2(g)} \tag{10}$$

During the NO_2 only period this model predicts that the platinum surface is almost completely covered by oxygen, which makes it difficult for propene to find vacant sites for adsorption. According to Burch and Sullivan [10], it is possible for propene in the gas phase to react directly with the oxygen on platinum, without the use of free platinum-sites. In the model we include two steps, where propene first adsorbs on Pt–O and forms an intermediate that reacts rapidly with other oxygen atoms on platinum to form $CO_{2(g)}$ and $H_2O_{(g)}$:

$$C_3H_{6(g)} + Pt–O \xrightarrow{r_{18}} Pt–O–C_3H_6 \tag{11}$$

$$Pt–O–C_3H_6 + 8Pt–O \xrightarrow{r_{19}} 9Pt + 3CO_{2(g)} + 3H_2O_{(g)} \tag{12}$$

Based on in situ FTIR experiments, Captain and Amiridid [19] also includes an oxygen activated hydrocarbon species in their mechanism for NO reduction by propene over Pt/SiO_2. Further, nitrates on barium are rather stable in inert gas, resulting in a quite slow desorption of NO_x, especially at 300 °C. The rate of desorption of NO_x stored in a Pt/BaO/Al_2O_3 sample is more rapid in the presence of propene [4]. We therefore suggest that the stored NO_x can react with CH_2 on platinum, which is shown in these two summation reactions:

$$3S_1\text{–}NO_2 + Pt\text{–}CH_2 \overset{r_{20}}{\rightarrow} 3NO_{(g)} + Pt + 3S_1 + CO_{2(g)} + H_2O_{(g)} \tag{13}$$

$$3Ba(NO_3)_2 + Pt\text{–}CH_2 \overset{r_{21}}{\rightarrow} 3NO_{(g)} + Pt + 3S_1\text{–}NO_3 + CO_{2(g)} + H_2O_{(g)} \tag{14}$$

When the reduction period ($NO_2 + C_3H_6$ mixture) is started, there is a NO breakthrough peak observed in the experiment (see Figs. 2 and 3) [5]. Thus, the NO_x is not completely reduced to N_2. This is the reason for the formation of $NO_{(g)}$, rather then $N_{2(g)}$ in the two reactions above. It would have been possible to include two extra reactions with formation of N_2 parallel to the NO formation, but we wanted to keep the number of reactions as low as possible. During the lean period in our experiments neither $CO_{2(g)}$ nor hydrocarbons are present in the inlet gas. However, during the reduction period $C_3H_{6(g)}$ is present in the gas phase and $CO_{2(g)}$ are formed, which results in carbonate formation, which have earlier been observed by in situ FTIR experiments [4]. In the model barium carbonate is formed by

$$CO_{2(g)} + S_1 \underset{r_{23}}{\overset{r_{22}}{\rightleftarrows}} S_1\text{–}CO_2 \tag{15}$$

It was assumed that there are repulsive interactions between carbonates in the same way as we assumed for nitrates [7] and therefore we let the activation energy for dissociation of carbonates, E_{23}, decrease with increasing coverage:

$$E_{23}(\theta) = E_{23}(0)(1 - \alpha_{23}\theta_{S_1\text{–}CO_2}) \tag{16}$$

where α_{23} is a constant. Carbonate formation has been observed to enhance the desorption of NO_x [12], but we did not have independent experiments of this phenomenon that could be used in the modelling procedure. Therefore, no further steps were added to the model to describe this promoting effect of CO_2.

Table 1 shows the observed amount of stored NO_x during 5 min of NO_2 exposure for two different pretreatments. This value was obtained by integrating the observed NO_x signal and subtracting this from the inlet value [4]. For the first pretreatment the catalyst was exposed to 500 ppm NO_2 and 1000 ppm propene and for the second pretreatment the catalyst was heated to 600 °C in N_2 only. The amount of stored NO_x is evidently enhanced if the catalyst is reduced with propene, even though it seems like the desorption of NO_x is complete at 600 °C [7]. There could be different explanations for this behaviour; hydrocarbon species may adsorb on the support (BaO and/or Al_2O_3) during the highly reducing atmosphere. An FTIR study [20] showed that propene adsorbs on an Al_2O_3 catalyst. Another explanation could be that the propene pulse is not square shaped giving some tailing after the propene is shut off. The propene from gas phase or the catalyst could then react with NO_x and reduce it to N_2. The catalyst may also be better regenerated when propene is used, compared to heating to 600 °C. In the model we chose to add a step where hydrocarbon species on platinum spill-over to the support. A new type of site for the support, S_2, was added, which could be Al_2O_3 or a combination of Al_2O_3 and BaO

Table 1
The amount of stored NO_x in a Pt/BaO/Al_2O_3 catalyst during 5 min of NO_2 exposure after two different pretreatments[a]

Temperature (°C)	NO_x storage (μmol/μmol Ba), pretreatment: NO_2 + propene	NO_x storage (μmol/μmol Ba), pretreatment: heating to 600 °C
300	0.28	0.18
400	0.29	0.16
500	0.19	0.07

[a] Pretreatment 1: 5 min 500 ppm NO_2 + 1000 ppm C_3H_6 at the reaction temperature shown in the table. Pretreatment 2: heated to 600 °C in N_2.

(BaO sites where NO_2 is not adsorbed):

$$\text{Pt–CH}_2 + \text{S}_2 \underset{r_{25}}{\overset{r_{24}}{\rightleftarrows}} \text{Pt} + \text{S}_2\text{–CH}_2 \tag{17}$$

The number of S_2 sites were determined by calculating the amount of S_2–CH_2 that was needed to explain the difference in storage between the two experiments. The result was 0.086 mol/kg catalyst. Finally, two more steps were added, where NO and NO_2 spill-over to the support and reacts with the adsorbed hydrocarbon compounds:

$$\begin{aligned}&\text{S}_2\text{–CH}_2 + 3\text{Pt–NO}_2\\&\quad\overset{r_{26}}{\rightarrow} 3\text{NO}_{(g)} + 3\text{Pt} + \text{S}_2 + \text{CO}_{2(g)} + \text{H}_2\text{O}_{(g)}\end{aligned} \tag{18}$$

$$\begin{aligned}&\text{S}_2\text{–CH}_2 + 3\text{Pt–NO}\\&\quad\overset{r_{27}}{\rightarrow} 3\text{Pt} + \text{S}_2 + \text{CO}_{2(g)} + \text{H}_2\text{O}_{(g)} + 1.5\text{N}_{2(g)}\end{aligned} \tag{19}$$

Figs. 2 and 3 show the results from the experiments and the simulations. In the upper panel of Fig. 2 the concentrations of NO, NO_2, NO_x and CO_2 are shown at 300 °C according to the experiments (solid lines) and the simulations (dotted lines), with 500 ppm NO_2 and altering between 0 or 1000 ppm C_3H_6. The lower panel shows the corresponding mean coverages on the surface according to the model. During the $C_3H_6 + NO_2$ phase, the coverage of CH_2 on platinum is high, as well as the coverage of carbonates on the barium oxide. When propene is shut off there is still some CO_2 production, probably due to dissociation of carbonates. In the model there is also CO_2 formation from reactions between NO_x and hydrocarbons adsorbed on the support. At the same time NO_2 starts to adsorb on BaO and the gas phase concentration of NO_x slowly increases as the coverage of BaO–NO_2 gradually saturates. In the third period of the experiment, the catalyst is again exposed to 1000 ppm C_3H_6 and 500 ppm NO_2. A breakthrough peak of NO is then observed [4]. The NO_x is rapidly desorbed from BaO and not completely converted to N_2. The model is able to describe this feature and the results are also shown in a magnification in Fig. 2. The simulated coverages in the lower panel also shows that the coverage of carbonates starts to increase again and also that CH_2 are adsorbed on the support. Fig. 3 shows the experimental and simulated concentrations for the corresponding experiments at 400 °C. The model is able to describe the main features in this experiment. Table 2 shows the kinetic parameters and the obtained value for α_{23} in Eq. (16) is -0.26.

Table 2

The kinetic parameters for the NO_x storage model for Pt/BaO/Al_2O_3[a]

Rate expression	A_i	$E_i(0)$ (kJ/mol)
$r_{13} = k_{13}C_{C_3H_6(g)}\theta_{v,Pt}$	$0.36^{b,d}$	7.3
$r_{14} = k_{14}\theta_{Pt–C_3H_6}$	$0.36^{c,d}$	179.7
$r_{15} = k_{15}\theta_{Pt–C_3H_6}\theta^2_{v,Pt}$	$2.3 \times 10^{9c,e}$	91.2
$r_{16} = k_{16}\theta_{Pt–CH_2}\theta_{Pt–O}$	$2.3 \times 10^{9c,e}$	89.1
$r_{17} = k_{17}\theta_{Pt–CH_2}\theta_{Pt–NO}$	$0.086^{c,d}$	188.5
$r_{18} = k_{18}C_{C_3H_6(g)}\theta_{Pt–O}$	$0.17^{b,d}$	11.2
$r_{19} = k_{19}\theta_{Pt–O–C_3H_6}\theta_{Pt–O}$	$2.3 \times 10^{9c,e}$	108.7
$r_{20} = k_{20}\theta_{Pt–CH_2}\theta_{S_1–NO_2}$	$0.055^{c,d}$	122.6
$r_{21} = k_{21}\theta_{Pt–CH_2}\theta_{Ba(NO_3)_2}$	$0.049^{c,d}$	120.6
$r_{22} = k_{22}C_{CO_{2(g)}}\theta_{v,S_1}$	$6.3 \times 10^{2b,d}$	19.7
$r_{23} = k_{23}\theta_{S_1–CO_2}$	$1.7 \times 10^{12c,e}$	159.2
$r_{24} = k_{24}\theta_{Pt–CH_2}\theta_{v,S_2}$	$0.15^{c,d}$	117.6
$r_{25} = k_{25}\theta_{S_2–CH_2}\theta_{v,Pt}$	$3.1 \times 10^{-8c,d}$	204.9
$r_{26} = k_{26}\theta_{S_2–CH_2}\theta_{Pt–NO_2}$	$7.0 \times 10^{2c,d}$	105.7
$r_{27} = k_{27}\theta_{S_2–CH_2}\theta_{Pt–NO}$	$0.096^{c,d}$	156.7

[a] A_i, $E_i(0)$, k_i and r_i denotes the pre-exponential factor, activation energy at zero coverage, rate constant and rate for a specific process, respectively. C_i and θ_i denotes the gas phase concentration and surface coverage for a certain species. $\theta_{v,Pt}$ is equal to $1 - \sum\theta_{i,Pt}$.

[b] Unit: m^3/(s kg catalyst).

[c] Unit: mol/(s kg catalyst).

[d] Centred pre-exponential factor (reference temperature: 600 K).

[e] Fixed to $10^{13}\ s^{-1}$.

5. Conclusions

Flow reactor studies combined with mean field kinetic modelling have been used to describe the NO_x storage phenomena on Pt/BaO/Al_2O_3. A kinetic model for a system like this includes many reaction steps. The complex system involving real exhaust and a commercial NO_x storage catalyst has in our investigations to various degrees been reduced to more simple systems: NO oxidation on Pt/Al_2O_3, NO oxidation on Pt/BaO/Al_2O_3, NO_x storage on BaO/Al_2O_3 and NO_x storage on Pt/BaO/Al_2O_3 with thermal or hydrocarbon regeneration. In this work, we focus on the NO_x storage on Pt/BaO/Al_2O_3 with regeneration using propene.

The kinetic models of NO oxidation on Pt/BaO/Al_2O_3 and NO_x storage on BaO/Al_2O_3, described in previous work, were used in the modelling of the NO_x

storage on the Pt/BaO/Al_2O_3 catalyst. The addition of platinum to the BaO/Al_2O_3 resulted in a promotion of the desorption of NO_x. In the model we described this phenomena with a spill-over step and the model agreed well with the experiments. Further, separate experiments were used to validate the model. In these experiments NO promoted the desorption of NO_x from the Pt/BaO/Al_2O_3 catalyst significantly. The model was able to describe this important feature, by reaction of NO with oxygen on platinum, resulting in NO_2 formation. This increased the number of free platinum-sites, which resulted in an increased spill-over of NO_x from the storage sites to platinum.

Experiments at 300 and 400 °C, with C_3H_6 and NO_2 were used to construct kinetic steps for the reduction with hydrocarbons. In the model the continuous reduction of NO_x occurs on platinum by a summation reaction between NO and hydrocarbon species on platinum. The rate of desorption of NO_x is higher when a hydrocarbon is present and in the model we describe this by a reaction between stored NO_x and CH_2 species on the surface. The model is able to describe the main features like reduction in rich atmosphere, the storage and breakthrough peaks in NO when switching from lean to rich mixture.

Acknowledgements

The work in this paper has been performed within the Competence Centre for Catalysis, which is financially supported by the Swedish National Energy Administration and the member companies: AB Volvo, Johnson Matthey-CSD, Saab Automobile AB, Perstorp AB, MTC AB, Eka Chemicals and Swedish Space Corporation.

References

[1] W. Bögner, M. Krämer, B. Krutzsch, S. Pischinger, D. Voigtländer, G. Wenninger, F. Wirbeleit, M.S. Brogan, R.J. Brisley, D.E. Webster, Appl. Catal. B 7 (1995) 153.

[2] N. Takahashi, H. Shinjoh, T. Iijima, T. Suzuki, K. Yamazaki, K. Yokota, H. Suzuki, N. Miyoshi, S. Matsumoto, T. Tanizawa, T. Tanaka, S. Tateishi, K. Kasahara, Catal. Today 27 (1996) 63.

[3] N. Miyoshi, S. Matsumoto, K. Katoh, T. Tanaka, J. Harada, N. Takahashi, K. Yokota, M. Sugiura, K. Kasahara, SAE Technical Paper Series No. 950809, 1995.

[4] E. Fridell, M. Skoglundh, B. Westerberg, S. Johansson, G. Smedler, J. Catal. 183 (1999) 196.

[5] E. Fridell, H. Persson, B. Westerberg, L. Olsson, M. Skoglundh, Catal. Lett. 66 (2000) 71.

[6] E. Fridell, H. Persson, L. Olsson, B. Westerberg, A. Amberntsson, M. Skoglundh, Top. Catal. 16–17 (2001) 133.

[7] L. Olsson, H. Persson, E. Fridell, M. Skoglundh, B. Andersson, J. Phys. Chem. B 105 (2001) 6895.

[8] R. Burch, T.C. Watling, Stud. Surf. Sci. 116 (1998) 199.

[9] R. Burch, T.C. Watling, Appl. Catal. B 11 (1997) 207.

[10] R. Burch, J.A. Sullivan, J. Catal. 182 (1999) 489.

[11] S. Balcon, C. Potvin, L. Salin, J.F. Tempère, G. Djéga-Mariadassou, Catal. Lett. 60 (1999) 39.

[12] A. Amberntsson, H. Persson, P. Engström, B. Kasemo, Appl. Catal. B 31 (2001) 27.

[13] L. Olsson, B. Westerberg, H. Persson, E. Fridell, M. Skoglundh, B. Andersson, J. Phys. Chem. B 103 (1999) 10433.

[14] M. Skoglundh, H. Johansson, L. Löwendahl, K. Jansson, L. Dahl, B. Hirschauer, Appl. Catal. B 7 (1996) 299.

[15] V.P. Zhdanov, Surf. Sci. Rep. 12 (5) (1991) 183.

[16] N.W. Cant, M.J. Patterson, Books of Abstract, Symposium No. 7, Proceedings of the Fifth European Congress on Catalysis, Limerick, Ireland, September 2–7, 2001.

[17] F. Zaera, Langmuir 7 (1991) 1998.

[18] F. Acke, M. Skoglundh, Appl. Catal. B 22 (1999) L1.

[19] D.K. Captain, M.D. Amiridid, J. Catal. 194 (2000) 222.

[20] V. Ermini, E. Finocchio, S. Sechi, G. Busca, S. Rossini, Appl. Catal. A 190 (2000) 157.